IMF Production in ^{64}Zn + ^{58}Ni at 35A-79A MeV

R. Wada, K. Hagel, J. Cibor, J. Li, M. Murray J. B. Natowitz, A. Ono[1]
and GANIL E160 collabolators

Production of intermediate mass fragments (IMF, $3 \leq Z \leq 15$) has been studied in ^{64}Zn + ^{58}Ni collisions at incident energies of 35, 49, 57, 69 and 79 MeV/nucleon. The experiment was performed at GANIL in France. Charged particles with Z $\leq$ 8 were detected by two plastic multidetectors, covering a total solid angle of 84% of 4π. Identification of Z=1 and 2 was made possible by the ΔE (or E) versus TOF method for particles with energy above 2.5A MeV. Identification of fragments ($3 \leq Z \leq 8$) was only possible for energies above 15-20A MeV in these detector arrays. In addition to the plastic multidetector arrays, five silicon telescopes were set at polar angles of $4.3^o, 7.3^o, 10.9^o, 16.0^o, 22.0^o$ and two at 28.5^o. The charges of all detected fragments in the telescopes were clearly identified and isotopes for $4 \leq Z \leq 7$ were also identified. More details of the experimental setup can be found in Ref.[1].

The experimental results have now been compared with an antisymmetrized molecular dynamics model (AMD-V)[2] calculations. For each energy about 2000 events have been generated in an impact parameter range of 0-8fm, which covers about 70% of the measured impact parameter range. The calculations have been done in the RIKEN VPP700 computer facility. The Gogny force,

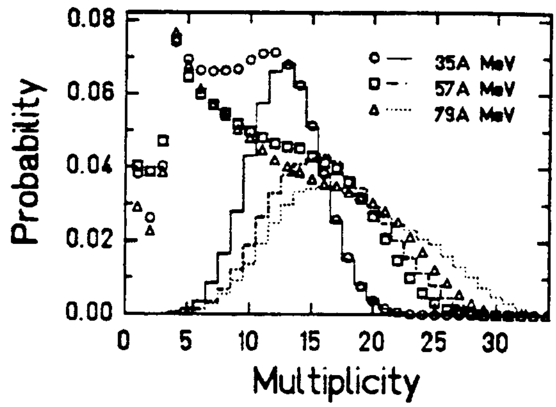

Figure 1: Multiplicity distribution of the observed charged particles. The calculated distributions (histograms) are obtained by filtering the events through the experimental conditions of detector angle coverages and energy thresholds. The calculated spectra are arbitrary normalized to the experimental distribution at each energy.

which gave the best fit in the previous analysis of ^{40}Ca+^{40}Ca at 35A MeV[3], was used in these simulations. The Gogny force gives an incompressibility of 228MeV for infinite nuclear matter. The generated fragments in AMD-V are generally in an excited state at a time of a few hundred fm/c (which corresponds to a realistic CPU time to calculate a few thousand events in VPP700) and it takes a further long time for the fragments to be cooled down. Instead of continuing the AMD-V calculation, the calculation was stopped at t=300fm/c and the fragments were cooled down, using a statistical decay code as an afterburner. The switching time is not crucial after t $\geq$ 200fm/c, because the excitation energy of the generated fragments drops sig-

[1] 1 Department of Physics, Tohoku University, Sendai, Japan

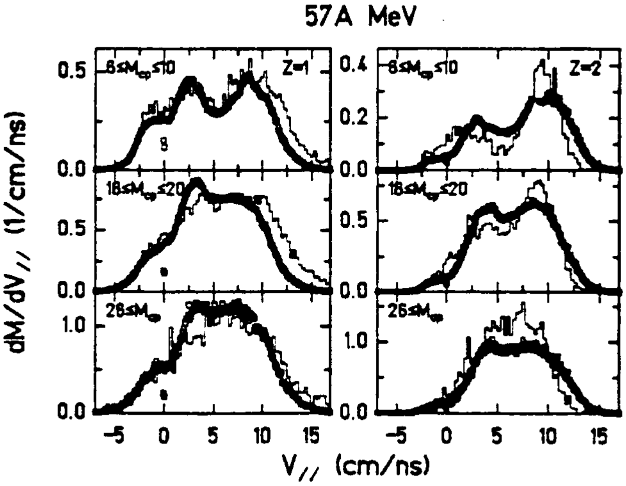

Figure 2: Parallel velocity distribution of Z=1 (left) and Z=2 (right) for different charged particle multiplicity windows. Experimental data are given by symbols and the calculated results are shown by histograms. The vertical scale is given in an absolute scale for both cases.

nificantly between 50fm/c and 200fm/c and it changes very slowly after freeze-out ($t \geq 200$fm/c). A modified version of GEMINI[4] was used as the afterburner. In this modified version the discrete levels of excited states of light fragments with $Z \leq 14$ are taken into account and the Hauser-Feshback formalism is extended to the particle decay with $Z \leq 20$ when the excitation energy of parent nuclei is below 50MeV. Each event generated by AMD-V is multiplied by a factor of 100 in the afterburner in order to get enough statistics to construct the final fragment energy spectra.

In Fig.1 total charged particle multiplicities are shown for three different incident energies. The experimental results are shown by symbols and the AMD-V results are shown by histograms. The calculated results are arbitrarily normalized to the experimental data. The high multiplicity side of the total measured events (about 50%) is reasonably reproduced for all incident energies.

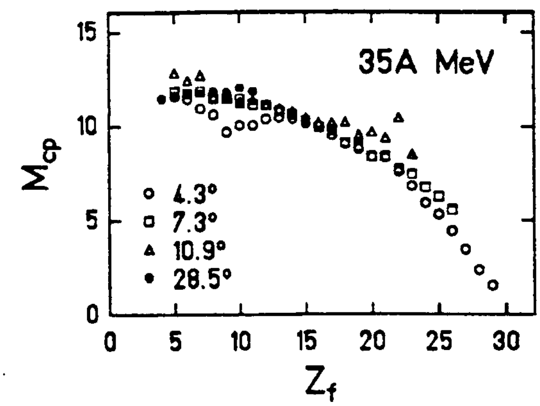

Figure 3: Experimental charged particle multiplicities are given as a function of the charge of the fragments detected in the Si telescopes at different angles.

In Fig.2 parallel velocities of Z=1 and 2 particles in the laboratory frame at 57A MeV are shown for three observed charged particle multiplicity windows. As seen in the figure, the simulated results (histograms) reproduce the essential features of the experimental results (open symbols). The relative yields of protons and alpha particles are also reasonably reproduced. For the low multiplicity window (upper figures), a two-peak structure is observed for both particles. The velocity corresponding to the higher peak is about 90% of beam velocity, which indicates that this component originates from a projectile-like source in binary type collisions. The velocity of the slower peak is near zero but not clearly determined because the spectra are deformed by the experimental conditions. The shoulder at $V_{//} \sim 0$ for Z=1 is caused by the shadow of the target frame, and the asymmetry of the two peaks for Z=2 is caused by the detector energy thresholds of the plastic arrays. For both particles the two peak structure gradually merges into a broad single bump when the multiplicity increases, suggesting that the contribution from an intermediate velocity source becomes important as the impact parameter of the collision decreases. This characteristic evolution of the parallel velocity distribution is observed for all incident energies studied here. This indicates that the charged particle multiplicity can be used as a reasonable indicator of the impact parameter of collisions.

In Fig.3 the average multiplicities of the observed charged particles (M_{cp}) are given as a function of the charge of the fragments detected in the Si telescopes for the reaction at 35A MeV. The calculated grazing angle is 2.9° at 35A MeV. At 4.3° fragments as heavy as Z=29 were observed. The heavy fragments have two energy components, one with a velocity close to the beam velocity and the other with a smaller velocity. (Heavy fragments with Z≥ 15 have only a high energy component because only those with enough energy to punch through the front ΔE Si (300 μm)

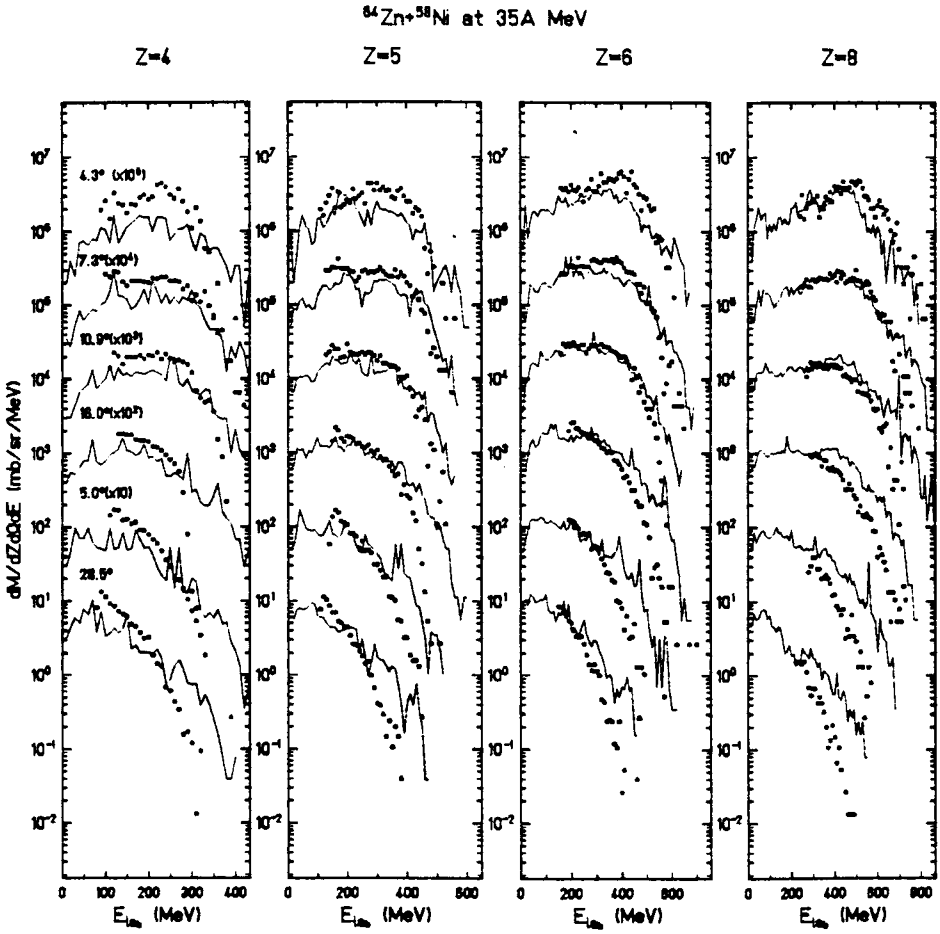

Figure 4: Energy spectra of Z=4, 5, 6 and 8 (from left to right) at different angles , indicating in the left figure, for the reaction at 35AMeV. Experimental data are shown by dots and the calculated spectra are shown by solid lines. The differential cross sections are given by an absolute scale for both experimental and simulated spectra. The spectra are multiplied by a factor of 10^n (n=0,1,2,3,4,5) from the bottom.

detector were Z identified.) A clear correlation is seen between the observed charged particle multiplicity and the charge of the fragments. This correlation is only slightly angle dependent. Intermediate mass fragments ($3 \leq Z \leq 15$) detected in the Si telescopes are associated with $M_{cp} \geq 10$ and no difference is observed between angles above 7.3^o, which suggests that the all observed IMF originate from a similar reaction mechanism. The similar trend is also observed for the results of the higher incident energies.

In Fig.4 inclusive energy spectra of Z=4, 5, 6, and 8 are plotted for the reaction at 35A MeV. The experimental data are shown by dots and the AMD-V results are shown by solid lines. All spectra are plotted in an absolute scale. The experimental scale is calculated from the total charge in a faraday cup. The absolute scale for the simulation is calculated from the impact parameter range. It should be noted that the calculated cross sections are from the impact parameter range of b=0-8fm and additional calculations for the larger impact parameter range may improve the fit for the spectra at forward angles. The experimental spectra are reasonably reproduced in shape and magnitude. For heavier fragments, however, the calculated spectra show slightly higher energy tail at the larger angles and this becomes more significant for the heavier fragments.

The AMD-V simulations reproduce the global features of the experimental results for the reactions studied here. Further AMD-V calculations for the larger impact parameter range are now underway. More detailed study in the experimental and calculated data may urther elucidate the reaction mechanism of the IMF production.

References

[1] J. C. Steckmeyer : *Phys. Rev. Lett.* **26**, 4895 (1996).

[2] A. Ono and H. Horiuchi : *Phys. Rev.* **C53**, 2958 (1996).

[3] R. Wada et al.: *Phys. Lett.* **B422**, 6 (1998).

[4] R. J. Charity et al.: *Nucl. Phys.* **A483**, 371 (1988).